Plasma Chemistry and Plasma Processing, Vol. 7, No. 3, 1987

Soft X-Ray Emission from a CO_2 Laser-Heated Z-Pinch Plasma

J. E. Tucker[1] and R. M. Gilgenbach[1]

Received August 7, 1986; revised February 25, 1987

We report results of soft X-ray measurements in which a high-power (10^{10}–10^{11} W/cm^2) CO_2 laser was used to heat a near critical density ($<10^{19}$ cm^{-3}) helium Z-pinch plasma. Frequency-integrated X-ray data show that the unheated Z-pinch plasma is Maxwellian with a temperature of about 30 eV. During laser heating, the X-ray emissions were enhanced over the unheated emissions. Analysis of the experimental X-ray spectra indicate that the low-energy portion of the X-ray emission spectrum (up to 600 eV) is enhanced over the baseline 30 eV Maxwellian emissions. This result is consistent with an inverse bremsstrahlung-modified distribution which results when the plasma heating rate is more rapid than the collisional thermalization rate. These results suggest that it may be possible to enhance the soft X-ray yield of a plasma lithographic source with laser heating.

KEY WORDS: Laser-heated Z-pinch plasma; helium; soft X-rays; plasma lithography.

1. INTRODUCTION

Soft X-ray sources have a number of important applications ranging from semiconductor processing[1] to X-ray microscopy.[2] Laser-heated targets have provided one source of soft X-rays,[3] whereas the gas-puff Z-pinch is now available commercially for soft X-ray generation. For certain applications it may be desirable to use a laser to control the soft X-ray spectrum from a Z-pinch. While a high-energy tail can be achieved in CO_2 laser–solid target interactions,[4] the enhancement of a low-energy soft X-ray component is less straightforward.

In this article we present results of soft X-ray measurements on a CO_2 laser-heated helium Z-pinch plasma. Our results show that laser heating of plasmas close to critical densities results in an enhancement of X-ray production in the lower-energy portion of the spectrum. This result is

[1] Intense Energy Beam Interaction Laboratory, Nuclear Engineering Department, University of Michigan, Ann Arbor, Michigan 48109.

0272-4324/87/0900-0365$05.00/0

consistent with existing models of inverse bremsstrahlung absorption of laser light.

2. EXPERIMENTAL

2.1. Configuration

This section describes the experimental configurations and diagnostics used to characterize the soft X-ray emission as a function of the electron temperature and density of the Z-pinch plasma, both with and without CO_2

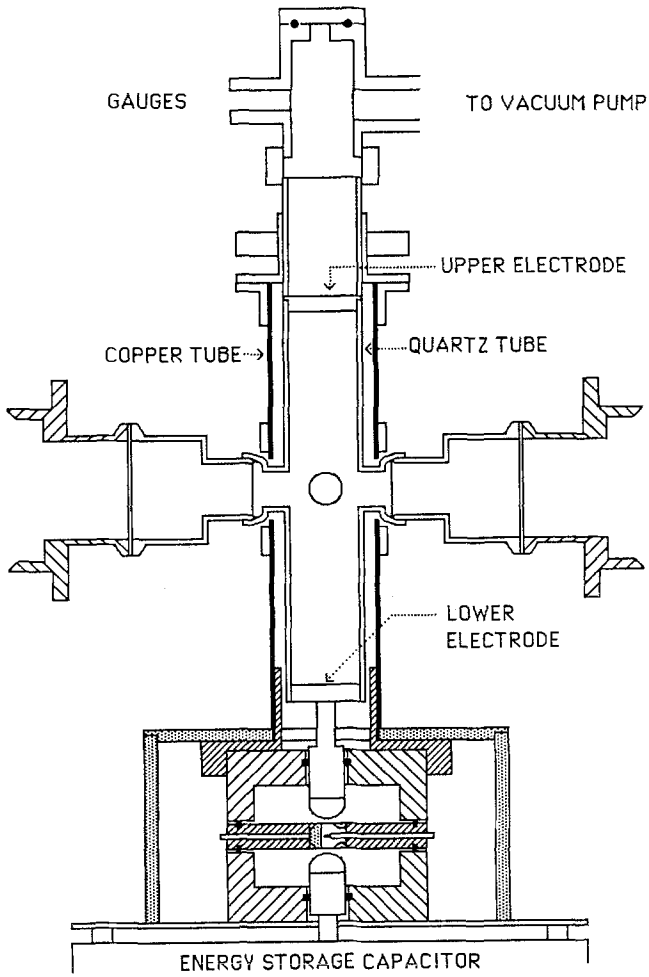

Fig. 1. Z-pinch configuration.

laser heating. The discharge was created inside a 3-cm-diameter quartz tube, 15 cm in length (Fig. 1). This high-current (~100 kA) discharge was driven by a low-inductance 13.4-μF energy storage capacitor which was charged to 14 kV. The discharge tube was evacuated to a base pressure of 5–20 mTorr and back-filled to an initial pressure of 2.6 Torr. Along the midplane of the discharge tube were four access holes of about 0.9 cm inner diameter. These holes allowed the soft X-ray and optical diagnostics to view the plasma and allowed the heating laser pulse access to the plasma.

The laser used for the heating experiments was a Lumonics 601 TEA CO_2 laser. The gain-switched pulse had an FWHM of 40 ns and a maximum energy of 16 J. The laser pulse was focused onto the center of the 0.2-cm-diameter plasma target through a modified Newtonian telescope with $f/6.8$ optics. At best focus, the focal spot was estimated to be approximately 150 μm.

2.2. Diagnostics

The diagnostics used to characterize the plasma were a frequency-integrated X-ray detector, an optical multichannel analyzer (OMA), a *p-i-n* diode, and a frequency-doubled ruby laser holographic interferometer. The CO_2 laser diagnostics were a germanium photon drag detector for the temporal occurrence of the pulse, and beam calorimeters for the incident and transmitted laser energy. A view of the experimental configuration for the CO_2 laser interaction experiments, as well as the location of the diagnostics, is shown in Fig. 2.

The X-ray detector consisted of a foil-filtered, fast plastic scintillator (NE102) connected through a 60-cm Lucite light guide to a high-gain bialkali photomultiplier tube (PMT Amperex model 2232B). Temporal resolution of the detector was approximately 10 ns. Aluminum foil filters with thicknesses that varied between 4.3 and 9 μm were used as the X-ray filters. These successfully blocked the plasma optical emissions from the PMT, while transmitting sufficient X-ray flux to give an acceptable signal-to-noise ratio. Due to the limited access to the plasma chamber, only one filtered PMT was used to view the plasma for these investigations. Thus, the results for different filter thicknesses were obtained on different discharges. The X-ray detector employed several different aperture sizes in an effort to reduce the extraneous X-ray emissions from wall interactions. The two aperture sizes used most often were 10.0 and 1.6 mm in diameter. Due to signal-to-noise restraints, most of the data were taken with a 1.6-mm aperture, which viewed a 0.9 cm segment of the plasma.

The OMA was used to characterize the plasma composition[5] and spatially averaged electron density by the Stark-broadened He II 468.6 nm

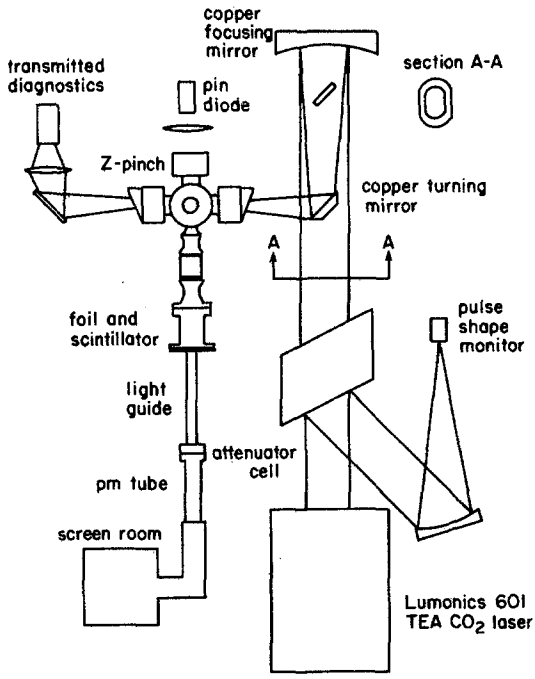

Fig. 2. CO_2 laser diagnostic configuration.

line. A *p-i-n* diode was used to measure the frequency-integrated visible light emissions from the pinch plasma. Frequency-doubled ruby laser holographic interferometry was used to provide spatially resolved electron densities of the unheated plasma. From holographic interferometric data, the peak plasma electron density was obtained at the time of the peak signal from the *p-i-n* diode signal (pinch time). Thus the *p-i-n* diode signal was used for all timing references in this paper. From these diagnostics, it was determined that the plasma was fully ionized and the peak electron density was near 10^{19} cm^{-3} at pinch time.

3. RESULTS

We first present X-ray data for the case of no laser heating. Figure 3 displays oscilloscope traces for the unheated plasma using a 4.3-μm aluminum filter. The typical signal from the X-ray detector had several emission maxima depending upon the aperture used on the detector. In particular, when the 10.0-mm aperture was used, there were only two emission peaks observed, while when any of the other apertures were used,

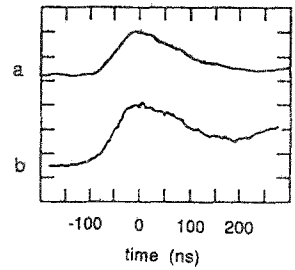

Fig. 3. Signals without laser heating: (a) *p-i-n* diode and (b) X-ray detector. Time scale is 50 ns per division.

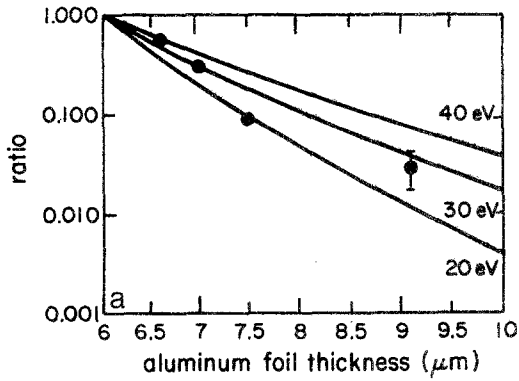

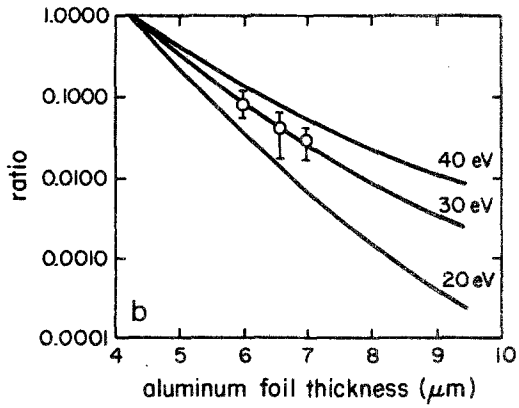

Fig. 4. Calculated ratio of frequency-integrated X-ray emissions and X-ray detector signal ratios from the Z-pinch plasma at pinch time: (a) 10.0 mm aperture, (b) 1.6 mm aperture.

the detector signal usually had three peaks. The first X-ray emission peak was from the pinched plasma and was the primary focus of this investigation. The maximum of the first X-ray emission peak occurred at the same time as the first *p-i-n* diode peak; thus both emission peaks occurred at the maximum plasma density. This X-ray emission peak had a width of about 200 ns above the background X-rays, and was approximately equal to the width of the visible light emission peak from the pinch plasma.

The X-ray emission spectrum from a thermalized plasma decreases with intensity as $\exp(-E/kT_e)$, where E is the X-ray energy and T_e is the electron temperature. For the case of the detector used in this experiment, the detector response will be a convolution of the plasma X-ray spectrum and the filter attenuation. Using an appropriate model of the plasma emissions (i.e., Maxwellian) and the attenuation coefficients of the filter, the X-ray detector response can be calculated for various plasma temperatures and filter thicknesses. By taking the ratio of the integrated X-ray flux through two foils, one can obtain values which can be compared to experimental data.[6]

The ratios of X-ray detector signals from several discharges with different foil thicknesses are shown in Fig. 4a for the 10-mm aperture, and in Fig. 4b for the 1.6-mm aperture for the peak X-ray detector signal at the first pinch. The ratios of the detector signal indicated that at pinch time, the plasma emissions were consistent with a Maxwellian distribution at a mean electron temperature of about 25–30 eV. This result is in good agreement with theoretical temperature estimates of 10–40 eV,[7] as well as the results from a similar Z-pinch experiment of 30–40 eV.[8]

3.1. Soft X-Rays from Laser-Heated Plasmas

The second aspect of these experiments concerned measurements to observe the enhancement of the plasma soft X-ray emissions from the plasma due to the absorption of the high-power CO_2 laser radiation.

The heating experiments proceeded by alternating the laser-heated discharges with the unheated discharges to ascertain the effects of the laser pulse on the pinch plasma. A set of the diagnostic signals for the laser-heated plasma is shown in Fig. 5. When enhanced X-ray emissions were seen, they temporally followed the intensity of the CO_2 laser pulse, indicating laser heating of the plasma. Figure 6 shows the unheated plasma X-ray detector signal for a 4.3-μm aluminum foil along with the laser-heated case for two different incident laser energies. Figure 7 presents soft X-ray data obtained for the same conditions as Fig. 6, except that the PMT filter was 6.0 μm aluminum. In the case of laser heating, the CO_2 laser pulse interacted with the plasma within 30 ns of pinch time.

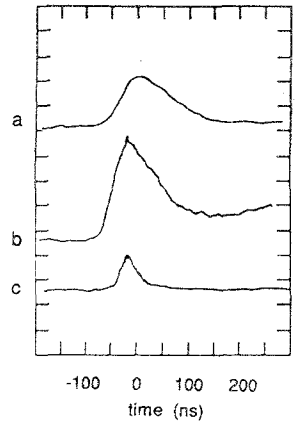

Fig. 5. Signals with laser heating: (a) *p-i-n* diode, (b) X-ray detector, and (c) laser power detector. Time scale is 50 ns per division.

An examination of Figs. 6 and 7 leads to several observations. First, there may exist a threshold energy between 1.4 and 6.4 J (corresponding to a vacuum intensity threshold of between 1 and 4.5×10^{11} W/cm^2) for the enhanced X-ray emissions to be observed. Second, the soft X-ray emission measurement results of the laser-heating experiments in general exhibited significant enhancement of the thin (4.3 μm Al) foil soft X-ray emissions from the plasma and less enhancement of the X-ray detector signal when a relatively thick filter (6 μm Al) was used. For a laser intensity of 4.5×10^{11}

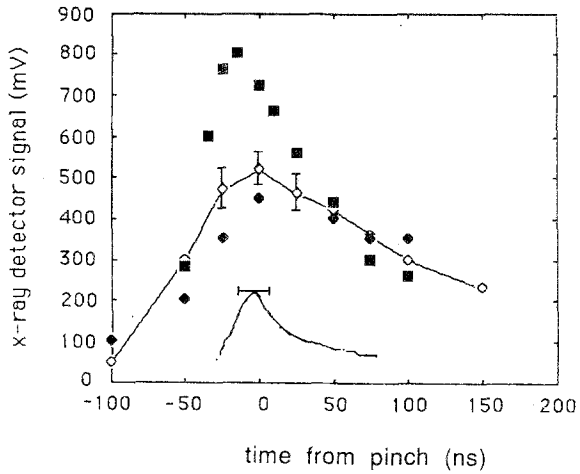

Fig. 6. Enhanced X-ray detector signal with laser heating for the case where the PMT filter was 4.3 μm aluminum. (◇) unheated plasma PMT signal; (◆) incident laser vacuum intensity of 1×10^{11} W/cm^2; (■) incident laser intensity of 4.5×10^{11} W/cm^2.

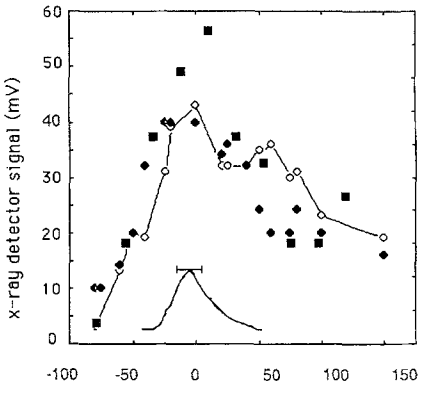

Fig. 7. Enhanced X-ray detector signal with laser heating for the case where the PMT filter was 6 μm aluminum. (◇) unheated plasma PMT signal; (◆) incident laser vacuum intensity of 1×10^{11} W/cm^2; (■) incident laser intensity of 4.5×10^{11} W/cm^2.

W/cm^2, it is seen that the CO_2 laser heating enhances the X-ray detector signal by about 60% over the unheated plasma signal for a 4.3-μm filter, whereas the X-ray detector signal was increased by about 20% for the 6.0-μm filter.

4. ANALYSIS AND DISCUSSION

The soft X-ray data for the two filter thicknesses can be examined to explore the absorption mechanisms for the laser energy by the plasma. The fact that the X-ray detector signal enhancement (and hence the frequency-integrated X-ray emissions from the plasma) was slightly higher for the thinner filter is an important result. If the dominant mechanisms for the absorption of the CO_2 laser light were through stimulated processes or resonance absorption, a very energetic component of the electron distribution would be generated.[4] If the plasma could be described by a two-temperature Maxwellian distribution with a high-energy tail, the PMT with thicker filters would see a larger increase of X-ray emissions over a thinner filter. We see the opposite effect: a slightly larger increase in the thin filter signal during laser heating relative to the increase in the thick filter signal.

The alternative view for the absorption mechanism for the CO_2 laser light by the plasma is that inverse bremsstrahlung (IB) is the dominant mechanism. In a system where IB is the dominant absorption mechanism of the radiation, an electron distribution can be created which has a larger low-energy population than does a Maxwellian distribution. This feature is a result of the decrease in the efficiency of IB as the electrons increase in energy. The expression for the attenuation of radiation by inverse

bremsstrahlung as it traverses a medium is

$$I(z) = I_0 \exp(-\kappa z) \tag{1}$$

where κ is the inverse bremsstrahlung coefficient and is given as

$$\kappa = \frac{\nu}{c\eta}\left(\frac{\omega_p^2}{\omega^2}\right) \tag{2}$$

in the limit where the electron–ion collision frequency ν is much greater then the wave frequency ω. In this expression, c is the speed of light, η is the index of refraction, ω_p is the plasma frequency, and the collision frequency is

$$\nu = Z\frac{e^2 m_e^{1/2}\omega_p^2}{4(kT_e)^{3/2}} \ln \Lambda \tag{3}$$

where m_e is the electron mass, e is the electron charge, Z is the ionic charge, and $\ln \Lambda$ is the Coulomb logarithm.

Theoretical models developed by Dum[9] and Langdon[10] have postulated that an IB-modified distribution can be created in plasmas where the laser heating rate is faster than the electron thermalization rate. This distribution function scales as $\exp(v/v_0)^5$, where v is the electron speed and v_0 is related to the electron temperature by[11]

$$kT_e = \frac{1}{\Gamma(0.6)} m_e v_0^2 \tag{4}$$

where $\Gamma(x)$ is the Gamma function. For the parameters of our experiment, this modified distribution can be created in the intensity range of 10^{11}–10^{12} W/cm^2. We examined this modified IB distribution by determining the modified bremsstrahlung and recombination radiation emission coefficients as a function of electron temperature and X-ray energy E in eV. The modified emission coefficients are, for bremsstrahlung,

$$j_b'(E) = \frac{48\pi}{3\sqrt{3}}\left(\frac{a\hbar}{m_e^{1/2}}\right)^3 n_e n_i Z^2 \left(\frac{1}{kT_e}\right)^{1/2} \Gamma\left(0.6, 0.134\left(\frac{E}{kT_e}\right)^{5/2}\right) \tag{5}$$

In this expression $\Gamma(\beta, \gamma)$ is the incomplete gamma function, n_i is the ion density, n_e is the electron density, and a is the fine-structure constant. In the case of large arguments, this function can be expanded in terms of the standard gamma function, which gives

$$j_b'(E) = \frac{133.6\pi}{3\sqrt{3}}\left(\frac{a\hbar}{m_e^{1/2}}\right)^3 n_e n_i Z^2 \frac{kT_e}{E^{3/2}} \exp\left[-0.134\left(\frac{E}{kT_e}\right)^{5/2}\right] \times\left(1 - 4.47\left(\frac{kT_e}{E}\right)^{5/2} + \cdots\right) \tag{6}$$

The recombination coefficients are similarly given as

$$j_r'(E) = \frac{11.4\pi}{3\sqrt{3}} \left(\frac{a\hbar}{m_e^{1/2}} \right)^3 n_e n_i Z^2 \frac{I_H}{n^3} \left(\frac{1}{kT_e} \right)^{3/2} \exp \left[-0.134 \left(\frac{E - I_{l,n}}{kT_e} \right)^{5/2} \right] \quad (7)$$

where I_H is the Rydberg constant and $I_{l,n}$ is in the ionization energy of the nth shell for the lth species.

An estimate of the expected temperature rise in the plasma was calculated in Ref. 12. Schmitt modeled the laser pulse absorption by the plasma in a fluid model for transient self-focusing. The associated heat transport problem was a strongly nonlinear differential equation and the electron temperature in the regions of the laser filamentation increased up to several hundred electron volts.

Using this calculated temperature rise for the heated plasma, the calculated X-ray emission intensities for a Maxwellian distribution at a temperature of 30 eV are compared to the modified IB distribution at a temperature of 150 eV, and are shown in Fig. 8. The intensities of Fig. 8 were multiplied by the X-ray filter attenuation factor as a function of X-ray energy to obtain the foil-transmitted spectra shown in Fig. 9. In Fig. 9, the dashed curves represent a 25-eV Maxwellian transmitted spectrum. The solid curves show the transmitted spectrum for the superposition of a 1% (heated) plasma volume fraction IB-modified distribution at 150 eV onto the 25-eV Maxwellian spectrum. The X-ray detector signal will be proportional to the frequency integral of this transmitted spectrum. As can be seen, the addition of the IB-modified spectrum enhances the signal transmitted through the 4.3-μm filter while only slightly enhancing the spectrum transmitted through the 6-μm filter. For this case, the integrated transmitted

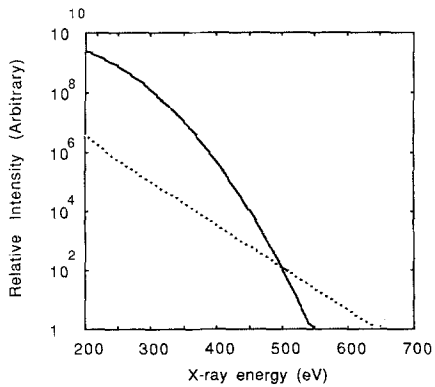

Fig. 8. Calculated emission intensities for a Maxwellian distribution at 30 eV (dashed line) and an IB-modified distribution at a temperature of 150 eV (solid line).

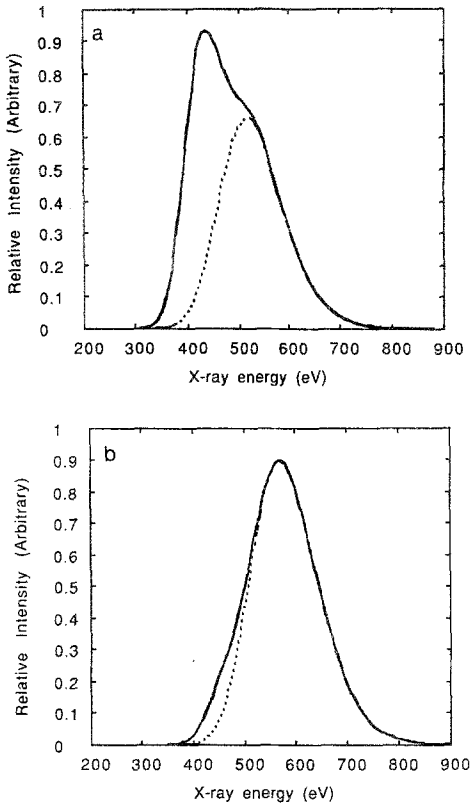

Fig. 9. Calculated X-ray transmission spectra for a 25-eV Maxwellian distribution (dashed line) and superposition of a 0.01 volume fraction of an IB-modified distribution at 150 eV onto the same distribution (solid line): (a) 4.3 μm Al filter; (b) 6.0 μm Al filter.

spectrum is increased by about 60% over the unheated spectrum for the 4.3-μm filter and by 10% for the 6-μm filter. This result is in reasonable agreement with the experimentally observed X-ray enhancement for similar plasma and laser conditions for the same foils (Figs. 6 and 7). Thus, the superposition of the IB-modified distribution onto the baseline plasma emissions can satisfactorily fit the experimental results.

5. CONCLUSIONS

The enhancement of the X-ray emissions from a near critical density plasma due to heating by a high-power CO_2 laser has been observed. The results of the frequency-integrated X-ray emission measurements cannot be fitted in terms of a bi-Maxwellian; they can be explained in terms of an

inverse bremsstrahlung-modified distribution superimposed onto the baseline Maxwellian plasma emissions. The threshold of the enhanced X-ray emissions was within a factor of 2–3 of the predicted threshold for the onset of the modified distribution function formation. By analysis of the experimental measurements, it was seen that the plasma X-ray emissions below about 600 eV were enhanced over the 30-eV Maxwellian baseline plasma emissions. Thus, it may be possible to use CO_2 laser heating to enhance the plasma emissions in the spectral region of interest for X-ray lithographic sources.

ACKNOWLEDGMENTS

This research was supported by National Science Foundation Grant No. ECS-8309682 and by the NSF Presidential Young Investigator Award No. ECS-8351837.

REFERENCES

1. I. Okada, Y. Saitoh, S. Itabashi, and H. Yoshihara, *J. Vac. Sci. Technol. B* **4**, 243 (1986).
2. R. Feder, J. S. Pearlman, J. C. Riordan, and J. L. Costa, *J. Microsc.* **135**, 347 (1984).
3. K. Koyama, T. Tomie, A. Yaoita, A. Matsushima, and M. Yano, Proc. of 6th Int. Conf on High-Power Particle Beams, Kobe, Japan, 1986.
4. B. Grek, H. Pepin, T. W. Johnson, J. B. Leboeur, and H. A. Baldis, *Nucl. Fusion* **17**, 1165 (1977).
5. J. E. Tucker, M. L. Brake, and R. M. Gilgenbach, *Appl. Phys. Lett.* **59**, 2251 (1986).
6. T. P. Donaldson, *Plasma Phys.* **20**, 1979 (1978).
7. J. G. Ackenhusen, Ph.D. Thesis, University of Michigan, Ann Arbor, Michigan (1977).
8. B. Hilko, J. Meyer, G. Albrecht, and H. J. Houtman, *Appl. Phys.* **51**, 4693 (1980).
9. C. T. Dum, *Phys. Fluids* **21**, 945 (1978).
10. A. B. Langdon, *Phys. Rev. Lett.* **44**, 575 (1980).
11. M. Lamoureux, C. Moller, and P. Jaegle, *Phys. Rev. A* **30**, 429 (1984).
12. A. J. Schmitt and R. S. B. Ong, *J. Appl. Phys.* **54**, 3003 (1983).